Journal of Power Sources 193 (2009) 769–773

Contents lists available at ScienceDirect

Journal of Power Sources

journal homepage: www.elsevier.com/locate/jpowsour

Short communication

A novel design and performance of cone-shaped tubular anode-supported segmented-in-series solid oxide fuel cell stack

Jiao Ding, Jiang Liu*

School of Chemistry and Chemical Engineering, South China University of Technology, The Key Laboratory of Enhanced Heat Transfer and Energy Conversation, Ministry of Education, Guangzhou 510641, PR China

ARTICLE INFO

Article history:
Received 10 March 2009
Received in revised form 22 April 2009
Accepted 23 April 2009
Available online 3 May 2009

Keywords:
Solid oxide fuel cell (SOFC)
Cone-shaped
Tubular
Segmented-in-series
Stack

ABSTRACT

A novel design of cone-shaped tubular segmented-in-series solid oxide fuel cell (SOFC) stack is presented in this paper. The cone-shaped tubular anode substrates are fabricated by slip casting technique and the yttria-stabilized zirconia (YSZ) electrolyte films are deposited onto the anode tubes by dip coating method. After sintering at 1400 °C for 4 h, a dense and crack-free YSZ film with a thickness of about 7 μm is successfully obtained. The single cell, NiO–YSZ/YSZ (7 μm)/LSM–YSZ, provides a maximum power density of 1.78 W cm^{-2} at 800 °C, using moist hydrogen (75 ml min^{-1}) as fuel and ambient air as oxidant.

A two-cell-stack based on the above-mentioned cone-shaped tubular anode-supported SOFC is fabricated. Its typical operating characteristics are investigated, particularly with respect to the thermal cycling test. The results show that the two-cell-stack has good thermo-mechanical properties and that the developed segmented-in-series SOFC stack is highly promising for portable applications.

1. Introduction

Solid oxide fuel cells (SOFCs) for portable application have attracted wide attention due to their high conversion efficiency, high waste-heat utilization, low pollution emission and practical fuel flexibility [1–6]. Generally, there are two main SOFC configurations, i.e. planar SOFC and tubular SOFC [7]. Planar SOFC is considered fragile and unable to endure the rapid heating and cooling needed for portable applications. In particular, the sealing layers need to be compatible with all the cell components; thus, most of the cell failures are imputable to a sealing problem [8,9]. However, tubular SOFC, because of its geometry, is capable of solving the problems related to cracking, sealing, thermal cycling, start-up/shut-down time and thermal shock resistance [10,11].

In the last few years, significant progress has been achieved in tubular SOFC development by Siemens Westinghouse. Some large-scale tubular SOFC demonstration units have been operated for increasing duration [12] and obtaining good cell performance. But for portable application, the small-scale tubular SOFC, with light weight and compact volume, is especially needed. Currently, many studies on SOFC have proved that small-scale tubular SOFC can endure thermal stress caused by rapid heating up to operating temperature. Small-scale tubular SOFC design enables cell stacks with high power density [13,14]. So, it is important to prepare small-scale SOFC stack with high electrochemical performance and long term stability for the portable application.

Liu [15] has been authorized a patent about a novel design of small-scale anode supported SOFC stack. This design of the SOFC configuration can increase the voltage and power of the stack while the volume of the stack is small. The patent also presented the characters of unit in the stack and connection method of the stack in detail. Sui and Liu [16] successfully made a three-cell-stack using electrolyte supported unit cell that demonstrated the feasibility of this design, though the power density was limited by large ohmic resistance from the thick electrolyte. Then Yuan et al. [17] prepared cone-shaped tubular anode-supported SOFC single cell and reduced the YSZ thickness by colloidal spray coating method in order to lower the ohmic resistance and improve the performance of the single cell. Zhang et al. [18] subsequently presented the preparation of anode-supported segmented-in-series SOFC stacks and obtained a much higher power density of the single cell than Yuan et al. [17]. But there is no electrochemical performance of the stack in their paper.

Based on these works above, we have made a two-cell-stack using cone-shaped tubular anode-supported single cell and investigated the performance of the stack. Furthermore, we have improved the microstructure of the anode and enhanced the performance of the single cell by adding AFL (anode functional layer), and we also have obtained the electrochemical performance of the stack especially the thermal cycling test. The results show that the two-cell-stack has good thermo-mechanical properties and that the

* Corresponding author. Tel.: +86 020 22236168; fax: +86 020 22236168.
E-mail address: jiangliu@scut.edu.cn (J. Liu).

0378-7753/$ – see front matter © 2009 Elsevier B.V. All rights reserved.
doi:10.1016/j.jpowsour.2009.04.049

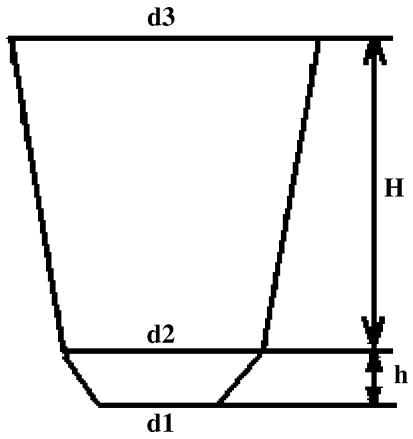

Fig. 1. The schematic diagram of the single cone-shaped tubular anode.

developed segmented-in-series SOFC stack is highly promising for portable applications.

2. Experimental

2.1. Preparation of NiO–YSZ cone-shaped tubular anode substrates

The fabrication procedure of the NiO–YSZ cone-shaped tubular anode substrates is similar to that described in our previous work [19–22]. The cone-shaped tubular anode substrates are prepared by slip casting technique. The schematic diagram of the single cone-shaped tubular anode is shown in Fig. 1. The as-prepared cone-shaped tubular anode substrates are pre-fired at 1000 °C for 4 h with a heating rate of 2 °C min^{-1}. After that, a NiO–YSZ layer which is called anode functional layer (AFL) is deposited onto the sintered anode tubes using dip coating method in order to form a homogeneous surface for coating electrolyte film. The slurry for the anode functional layer is composed of NiO (synthesized by glycine-nitrate process), YSZ (TZ-8Y, Tosoh corporation, Tokyo, Japan), ethylcellulose (A.R., Dongfeng Chemical Reagents Plant, Wenzhou, China), terpineol (A.R., Tianjin Kermel Chemical Reagents Development Centre, Tianjin, China), oil and ethanol. The detailed slurry composition for anode functional layer has been reported elsewhere [19].

2.2. YSZ electrolyte deposition and sintering

The YSZ electrolyte films are deposited onto the cone-shaped tubular anodes using dip coating technique [21,23]. YSZ powder bought from Tosoh corporation (TZ-8Y, Tosoh corporation, Tokyo, Japan) is chosen to make thin electrolyte film in this study. Fine YSZ particles are mixed with ethanol by ultrasonic for 30 min to form uniform and stable YSZ suspension. Additionally, terpineol and ethylcellulose are added as plasticizer and binder, respectively. Firstly, the outside surface of the cone-shaped tubular anode is put into the YSZ suspension for 10 s. Then the anode/electrolyte bilayers are drying using a hair drier in the open air. Dip coating and subsequent drying are performed several times to reach a required electrolyte thickness. Then, the anode/electrolyte bilayers are sintered at 1400 °C for 4 h to densify the YSZ films.

2.3. Single SOFC fabrication and testing

LSM (60 wt%)–YSZ composite cathode paste and pure LSM cathode current collector layer are applied onto the YSZ electrolyte film by slurry coating and finally sintered at 1200 °C for 2 h. Silver paste

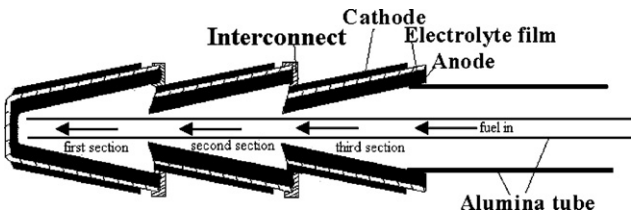

Fig. 2. Schematic diagram of a cone-shaped tubular segmented-in-series SOFC stack.

(Shanghai Research Institute of Synthetic Resins, Shanghai, China) is used as the current collector for both anode and cathode. A four-probe testing set-up is adopted to eliminate the ohmic loss in the silver wires. The single cone-shaped tubular SOFC is attached to one end of an alumina tube with the anode inside by using silver paste as sealing and jointing material [24–26]. Hydrogen saturated with water at room temperature (3% water) is used as fuel at the anode side at a flow rate of 75 ml min^{-1} and ambient air is used as oxidant at the cathode side. The cell is tested in the temperature range of 600–800 °C.

2.4. Assembling of the segmented-in-series SOFC stack

Fig. 2 is the schematic diagram of the cone-shaped tubular segmented-in-series SOFC stack. A short period SOFC stack is composed of several sections of cone-shaped tubular single SOFC fabricated by slip casting technique and dip coating method. As can be seen from Fig. 2, the cone-shaped tubular single cells are fitted one into the other to form a stack. They are connected in electrical and gas flow series. The interconnect serves as sealing and electrical connection between the anode of one single cell and the cathode of the next single cell.

Fig. 3 shows the photo of the as-prepared two-cell stack. The two-cell-stack is assembled by connecting two of the cone-shaped tubular single cells in electrical and gas flow series [15,18]. The smaller end of the first cell is closed, while the bigger end of the first cell and both ends of the second cell are open. Silver paste serves as sealing and electrical connection [24–26] is applied in the joint part to connect the two single cell units by invaginating the smaller end of the second cell into the bigger end of the first cell. Then the as-prepared stack is heated at 500 °C for 2 h with a heating rate of 2 °C min^{-1} to evaporate the solvent and binder in the silver paste in order to densify the connection. The assembled two-cell-stack is attached to one end of an alumina tube with the anode inside. Hydrogen (75 ml min^{-1}) saturated with water at room temperature (3% water) is used as fuel at the anode side and ambient air is used as oxidant at the cathode side. The two-cell-stack is tested in the temperature range of 600–800 °C. Thermal cycling tests are performed for the two-cell-stack. For each period of thermal cycling test, the

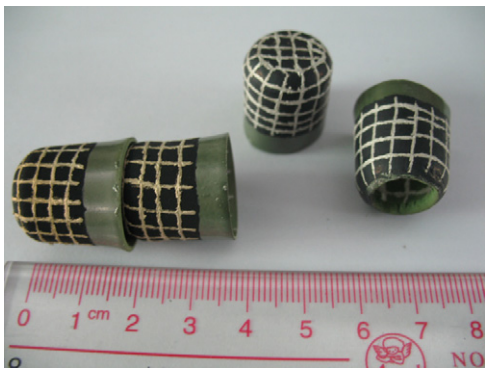

Fig. 3. Photo of a two-cell-stack.

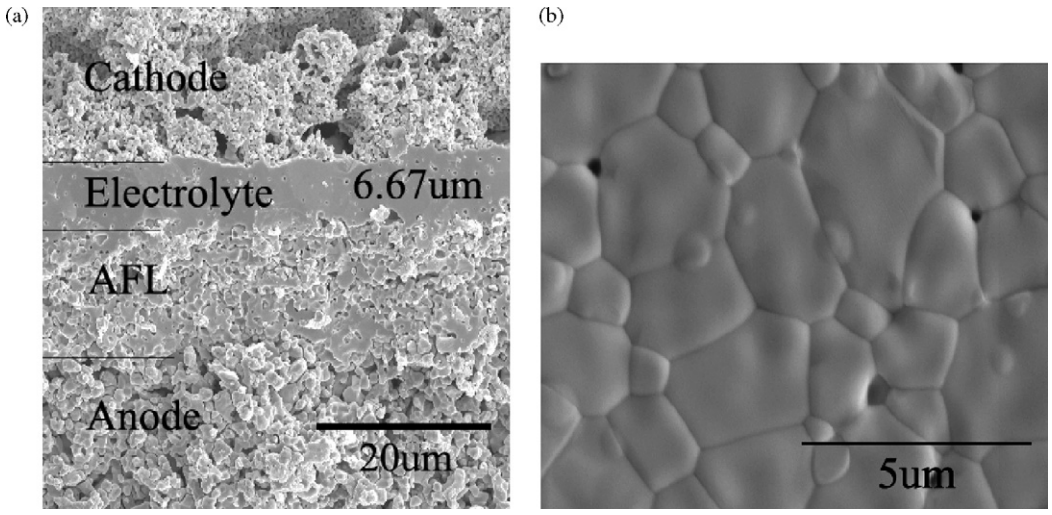

Fig. 4. Microstructure of the cell section and surface of the YSZ film. (a) Cross-sectional image of a region showing anode, AFL, electrolyte, cathode. (b) Surface view of YSZ film sintered at 1400 °C.

temperature of the two-cell-stack is increased from room temperature to 800 °C, holding for about half an hour, testing the stack performance, and then lowered to room temperature. Finally, the testing of the two-cell-stack is shut down to wait another thermal cycling test another day. In another day, the testing of the two-cell-stack is start up again from room temperature. The total effective area of the two-cell-stack is 10.65 cm^2 including 7.80 cm^2 of the first cell and 2.85 cm^2 of the second cell.

3. Results and discussion

3.1. Microstructure of as-prepared samples

Fig. 4 shows the microstructure of the cell section and surface of the YSZ film. Fig. 4(a) is a representative fracture cross-sectional SEM image of the single cell, showing a 7 μm-thick YSZ film has been successfully coated on the anode. As can be seen, the electrode layers are with the expected porosity while the YSZ electrolyte film is quite dense and without any cracks or delaminations. All the layers are reasonably flat and uniform, with intimate contact at the interfaces.

The thickness of the anode functional layer (AFL) is about 15 um. The AFL is relatively dense compared to the porous anode substrate, and it can be considered as the transition from the anode to the electrolyte. Two functions are expected from the AFL. First, a fine thinner YSZ electrolyte film can be obtained on the less porous AFL layer so that the ohmic resistance of the cell can be reduced. Second, the introduction of the AFL increases the triple phase boundary (TPB) area, so that decreases the polarization of the anode. Both functions are critical in improving the performance of the cell.

Fig. 4(b) is a surface view of sintered YSZ film. It can be seen that the YSZ film is composed of irregular grains without cracks.

3.2. Electrochemical performance of the single cell

Fig. 5 shows the *I–V–P* characteristics of a single cell operated at different temperatures using moist hydrogen (75 ml min^{-1}) as fuel and ambient air as oxidant. As can be seen, the performance of the single cell is encouraging, providing a maximum power density (MPD) as high as 1.78 W cm^{-2} at 800 °C, more than three times of that obtained from a similar cell without AFL [17]. As mentioned above, the electrochemical property of the single cell is improved by introducing the thin and relatively dense AFL. These results are also better than those of SOFCs that used the same single cell structure of

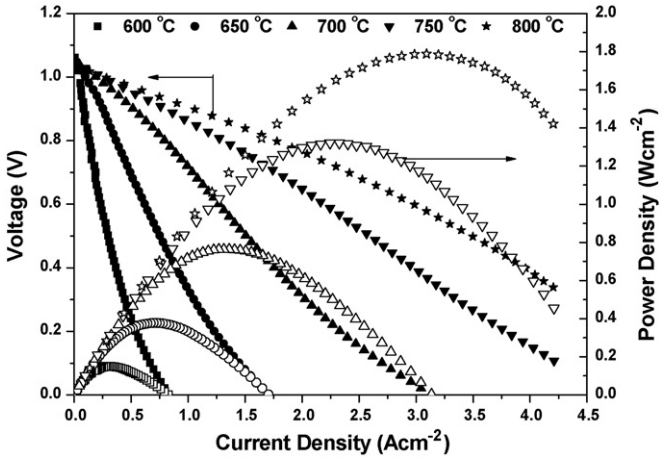

Fig. 5. *I–V–P* characteristics of a single cell operated at different temperatures using moist hydrogen as fuel and ambient air as oxidant.

NiO–YSZ/YSZ/LSM–YSZ without AFL, and the detailed comparison is shown in Table 1. It can be seen that the YSZ film of the present cell is the thinnest by introducing AFL and the single cell can provide the highest power density among the cells listed in Table 1 [27–29].

Fig. 6 shows the impedance spectra of the cell at 750 °C and 800 °C. As can be seen from the impedance spectra, the interfacial polarization resistance dominates the total resistance of the cell while the ohmic resistance is very small. This result reveals that the ohmic resistance of the cell with 7 μm-thick YSZ electrolyte film is very small and such thin YSZ film is very dense without

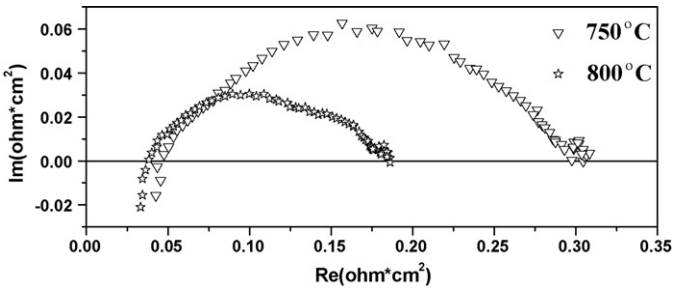

Fig. 6. Impedance spectra of single cell operated at 750 °C and 800 °C.

Table 1
Comparison of the maximum power density between the present cell and prior reported cells of Ni–YSZ/YSZ/LSM–YSZ at 800 °C.

References	Cell structure	YSZ Film thickness (μm)	Interfacial polarization resistance (Ω cm^2)	Interfacial polarization resistance/whole resistance (%)	MPD at 800 °C (W cm^{-2})
[27]		25	0.29	70	1.03
[28]	NiO–YSZ/YSZ/LSM–YSZ	10	0.31	88	1.40
[29]		31	0.5	90	0.97
This study		7	0.15	81	1.78

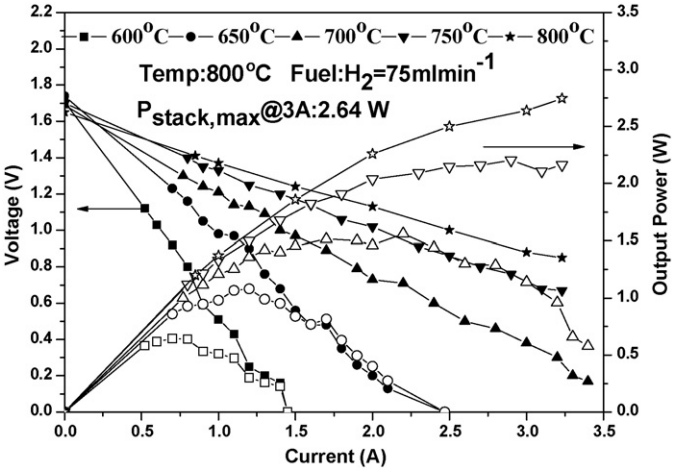

Fig. 7. *I–V–P* characteristics of the two-cell-stack operated at different temperatures using moist hydrogen as fuel and ambient air as oxidant.

crack or defect by introducing the relatively dense AFL. Furthermore, from Table 1, we can see more clearly that the interfacial polarization resistance of present cell is the smallest. This indicates that the microstructure of the electrode and the interfacial of the electrode/electrolyte of our present cell are greatly improved. However, compared with the ohmic resistance, the interfacial polarization resistance is still big and it dominates the total resistance of the cell. The result reveals that further improvement of electrode is very necessary and should be strived for in future studies.

3.3. Electrochemical performance of the two-cell-stack

Fig. 7 shows the performance of the two-cell-stack operated at different temperatures using moist hydrogen as fuel and ambient air as oxidant. The stack presents an open circuit voltage (OCV) of about 1.7 V and a maximum output power of >2.75 W at 800 °C. This indicates that the OCV of each unit cell is about 0.85 V at 800 °C, substantially lower than the theoretical value of ≈1.1 V per cell in humidified hydrogen and ambient air. Furthermore, the two-cell-stack presents a maximum power density (MPD) as 0.258 W cm^{-2} at 800 °C, much lower than the single cell showed in Fig. 5. Because the working potential of the two-cell stack is lower than that of the algebraic sum of theoretic potential of two single cells. Besides, the effective area of the two-cell-stack is much larger than the single cell so that the route of current becomes longer which results in the larger resistance.

Fig. 8 shows the performance of each cell in the two-cell-stack at 800 °C. It can be seen that the OCV of each cell in the stack is lower than the single cell in Fig. 5. Furthermore, the maximum power density (MPD) of the first cell at 800 °C is 0.22 W cm^{-2} while that of the second cell is 0.33 W cm^{-2}, much lower than that of the single cell described before (1.78 W cm^{-2} at 800 °C). These results can be explained by two reasons. First of all, the preparation technique of

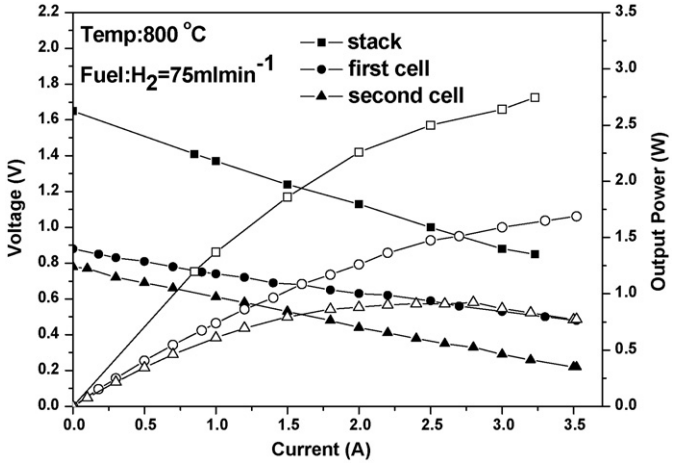

Fig. 8. Performance of the cells composing two-cell-stack at 800 °C.

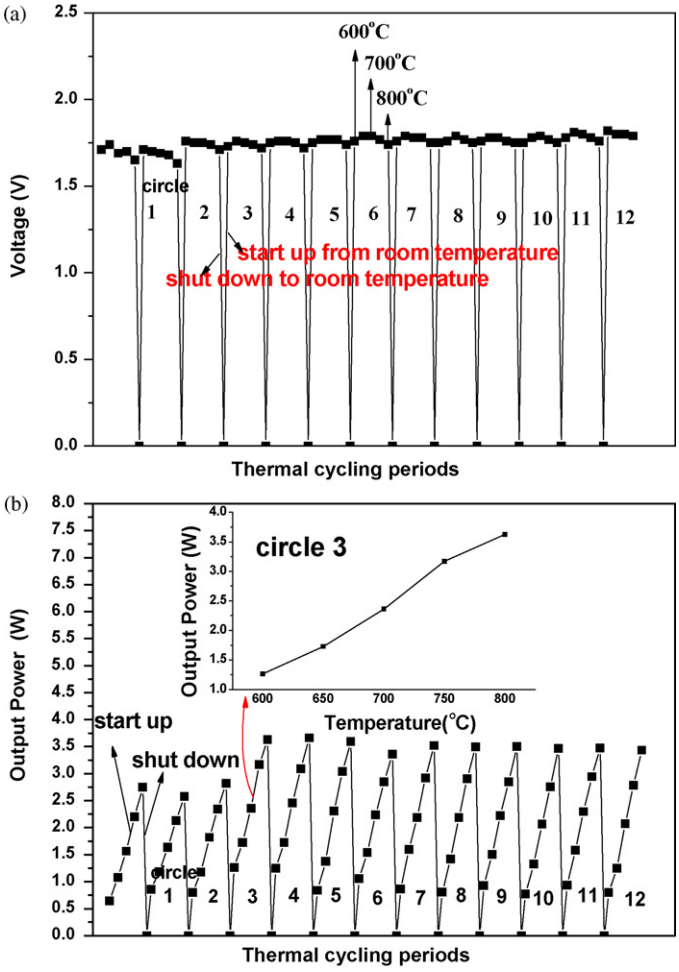

Fig. 9. Thermal cycling stability of the two-cell-stack (a) the OCV change with the thermal cycling periods (b) the output power change with the thermal cycling periods.

each cell is not so stable that causes the OCV and electrochemical performance of the cell units consisted the stack are not identical. Secondly, the low OCV and MPD of the cell units in the stack may be attributed to gas leakage across the Ag paste sealing at the connection. However, it should not be the problem of Ag sealing material, while the gas leakage may be caused by improper operation of applying techniques for sealing. There are lots of literatures and patents confirming the feasibility of silver seals and silver leads used in IT (intermediate temperature, 600–800 °C) SOFC [24–26]. And Ag paste is a kind of simple, fast and effective sealing material for transitory use. However, from the view point of long-term stability and reliability, Ag is not a suitable sealing material for SOFC. Because the melting point of Ag is about 960 °C and it will evaporates at the temperatures SOFC works. Besides, Ag can react with H_2 fuel to induce hydrogen fragile, which results in failure of sealing. Actually, some converted sealing materials, such as lanthanum chromite based compounds, are being considered for long term sealing use. Some literatures [30–34] have reported this kind of material used for sealing and current-collecting.

3.4. Thermal cycling stability of the two-cell-stack

Fig. 9 shows the electrochemical behavior of a SOFC after twelve periods of thermal cycling test. As shown in Fig. 9(a), the stack OCV does not change significantly, and the overall stability is good after twelve periods thermal cycling tests. Moreover, after the first thermal cycling test, the stack OCV is a little higher than before, which can be attributed to the anode which is not completely reduced at the first time testing. Stability of the stack OCV demonstrates feasibility of the cone-shaped segmented-in-series design. It can be seen from Fig. 9(b), the output power increases after twice thermal cycling tests and then it is stable with no apparent cycle-to-cycle degradation. These indicate that the as-prepared two-cell-stack can endure thermo-mechanical stresses through the thermal cycling test and this character is very significant for portable application.

4. Conclusions

A new design of cone-shaped tubular segmented-in-series solid oxide fuel cell (SOFC) stack is presented in detail in this paper. The cone-shaped tubular anode substrates are fabricated by slip casting technique and the yttria-stabilized zirconia (YSZ) electrolyte films are deposited onto the anode by dip coating method. The single cell, NiO–YSZ/YSZ (7 μm)/LSM–YSZ, provides a maximum power density of 1.78 W cm^{-2} at 800 °C using moist hydrogen as fuel and ambient air as oxidant.

A two-cell-stack based on our design of cone-shaped tubular anode-supported SOFC is successfully fabricated. The as-prepared two-cell-stack is able to withstand at least twelve periods of thermal cycling test without failure. This shows that the as-prepared SOFC stack has good thermo-mechanical properties and that the developed SOFC stack is a highly promising SOFC stack for portable applications.

Further investigation on the stack will be conducted, such as adopting innovative sealing materials and current-collecting materials, improving the microstructure of electrode, finding possible stack improvements and optimizing operating conditions, using the hydrocarbon fuel, and so on. Our final aim is to construct segmented-in-series stack for SOFC portable application, which is now ongoing.

Acknowledgement

Financial support from the National “863” program of china (grant No. 2007AA05Z136), the Department of Science and Technology of Guangdong Province (grant No. 2005B50101007) and Department of Education of Guangdong Province (grant No. B15-N9060210) are gratefully acknowledged.

References

[1] N.Q. Minh, J. Am. Ceram. Soc. 76 (1993) 563–588.
[2] Y. Zhang, S. Zha, M. Liu, Adv. Mater. 17 (2005) 487–491.
[3] B.C.H. Steele, Nature 400 (1999) 619–621.
[4] G.A. Tompsett, C. Finnerty, K. Kendall, T. Alston, N.M. Sammes, J. Power Sources 86 (2000) 376–382.
[5] S.C. Singhal, Solid State Ionics 152–153 (2002) 405–410.
[6] J.M. Wang, Z. Lu, X.Q. Huang, K.F. Chen, N. Ai, J.Y. Hu, W.H. Su, J. Power Sources 163 (2007) 957–959.
[7] N.M. Sammes, Y. Du, R. Bove, J. Power Sources 145 (2005) 428–434.
[8] M. Stelter, A. Reinert, B.E. Mai, M. Kuznecov, J. Power Sources 154 (2006) 448–455.
[9] T. Suzuki, T. Yamaguchi, Y. Fujishiro, M. Awano, J. Power Sources 160 (2006) 73–77.
[10] I.P. Kilbride, J. Power Sources 61 (1996) 167–171.
[11] N.M. Sammes, Y.H. Du, Int. J. Appl. Ceram. Technol. 4 (2) (2007) 89–102.
[12] R.A. George, J. Power Sources 86 (2000) 134–139.
[13] Y. Funahashi, T. Shimamori, T. Suzuki, Y. Fujishiro, M. Awano, J. Power Sources 163 (2007) 731–736.
[14] M. Lockett, M.J.H. Simmons, K. Kendall, J. Power Sources 131 (2004) 243–246.
[15] J. Liu, Chinese Patent: CN100347897.
[16] J. Sui, J. Liu, ECS Trans. 7 (1) (2007) 633–637.
[17] W.S. Yuan, J. Liu, J. Sui, Y.H. Zhang, Chin. J. Power Sources 32 (7) (2008) 446–448.
[18] Y.H. Zhang, J. Liu, J. Yin, W.S. Yuan, J. Sui, Int. J. Appl. Ceram. Technol. 5 (6) (2008) 568–573.
[19] J. Ding, J. Liu, W.S. Yuan, Y.H. Zhang, J. Eur. Ceram. Soc. 28 (2008) 3113–3117.
[20] J. Ding, J. Liu, J. Am. Ceram. Soc. 91 (10) (2008) 3303–3307.
[21] J. Yin, J. Liu, Y.H. Zhang, Chin. J. Power Sources 32 (12) (2008) 835–837.
[22] J. Liu, Y.H. Zhang, J. Sui, W.S. Yuan, J. Yin, J. Ding, Chinese Patent: ZL 2007 1 0031105.3.
[23] Y.H. Zhang, J. Liu, Chinese Patent: ZL 2007 1 0031104.9.
[24] J. Liu, Z. Lv, S.A. Barnett, Y. Ji, W.H. Su, in: S.C. Singhal (Ed.), Proceeding of the 9th International Symposium on Solid Oxide Fuel Cells, Electrochemical Society Proceedings Volume 2005–07, 2005, pp. 1976–1980.
[25] J. Liu, S.A. Barnett, Solid State Ionics 158 (2003) 11.
[26] J. Liu, W.H. Su, Z. Lv, Y. Ji, L. Pei, W. Liu, T.M. He, Chinese Patent: CN1180493.
[27] J. Liu, S.A. Barnett, J. Am. Ceram. Soc. 85 (12) (2002) 3096–3098.
[28] Y.H. Zhang, X.Q. Huang, Z. Lv, Z.G. Liu, X.D. Ge, J.H. Xu, X.S. Xin, X.Q. Sha, W.H. Su, J. Am. Ceram. Soc. 89 (7) (2006) 2304–2307.
[29] Y.H. Zhang, X.Q. Huang, Z. Lv, X.D. Ge, J.H. Xu, X.S. Xin, X.Q. Sha, W.H. Su, Solid State Ionics 177 (2006) 281–287.
[30] H. Yoshida, H. Yakabe, K. Ogasawara, T. Sakurai, J. Power Sources 157 (2006) 775–781.
[31] X.L. Zhou, P. Wang, L.M. Liu, K.N. Sun, Z.Q. Gao, N.Q. Zhang, J. Power Sources (2009), doi:10.1016/j.jpowsour.2009.02.071.
[32] N. Shaigan, D.G. Ivey, W.X. Chen, J. Power Sources 185 (2008) 331–337.
[33] M.F. Liu, L. Zhao, D.H. Dong, S.L. Wang, J.D. Wu, X.Q. Liu, G.Y. Meng, J. Power Sources 177 (2008) 451–456.
[34] X.L. Zhou, F.J. Deng, M.X. Zhu, G.Y. Meng, X.Q. Liu, J. Power Sources 164 (2007) 293–299.